Research Article

Tintin Mutiara, Hary Sulistyo, Moh. Fahrurrozi, and Muslikhin Hidayat*

Facile route of synthesis of silver nanoparticles templated bacterial cellulose, characterization, and its antibacterial application

https://doi.org/10.1515/gps-2022-0038
received October 30, 2021; accepted March 09, 2022

Abstract: Bacterial cellulose (BC) produced from coconut water, commonly known as *nata de coco*, is a biopolymer with enormous properties. Compared to plant cellulose, BC has better mechanical strength and a greater degree of polymerization. BC's high purity and high porosity make it a suitable candidate for the embedding and dispersion template for silver nanoparticles (AgNPs). This study investigated a facile and scalable method of making BC from coconut water and impregnated them with $AgNO_3$ solution to produce AgNPs templated BC. The resulting materials were characterized by Fourier transform infra-Red (FTIR), scanning electron microscope (SEM), energy dispersive X-ray (EDX), and X-ray diffraction (XRD). The thermal stability was also investigated by thermogravimetric analysis (TGA). The antibacterial activity of AgNPs templated BC was challenged in cultures of gram-positive bacteria *Staphylococcus aureus* and gram-negative bacteria *Escherichia coli* and showed an inhibition zone of growth in agar media. This study proves that the resulting AgNPs templated BC sheets are potential materials for antibacterial and industrial application that are low cost and easy to produce.

Keywords: antibacterial, bacterial cellulose, characterization, silver nanoparticles

1 Introduction

As the most common biopolymer material with a production of 1.5×10^{12} tons per year, cellulose is considered an unlimited source of raw material, which has the potential to increase the need for biocompatible and environmentally friendly products [1]. Compared to plant cellulose, bacterial cellulose (BC) has several superior characteristics such as high purity, high porosity, high water retention capacity, high crystallinity, better mechanical strength, and fibers of BC have a high aspect ratio [2]. Cellulose produced from bacteria (such as *Acetobacter xylinum*, *Gluconacetobacter hansenii*, and *Gluconacetobacter medellinensis* [3,4]) has abundant hydroxyl groups making it a material that has high biocompatibility [3–5], which is easy to combine with other materials to form a composite. In addition, the structure of BC has extraordinary mechanical strength and a high specific surface area [5]. Recent studies have shown improvements in the mechanical [6], hydrophilicity [1], durability [7], and antibacterial [8–10] properties of BC composite via chemical and surface modification. Some of the most exciting applications of BC as a biomaterial is the wound dressing, temporary skin substitute, antibacterial textile, and sterile package. In these applications, the antibacterial properties of BC become the most crucial properties to be obtained. Because of the high biocompatibility, BC is considered as a suitable matrix for the assimilation of metals. Among the several metals that could be inserted in the BC matrix, silver has drawn interest due to the wellknown antibacterial properties.

Nanoparticles with a size range between 1 and 100 nm show various improved properties compared to bulk form due to changes the in shape, size, size distribution, and surface area [11]. Various specific applications of nanoparticles refer to their large surface area for chemical reactions [12]. The antibacterial characteristics of silver nanoparticles (AgNPs) are much improved compared to the bulk form due to the increased physicochemical and mechanical properties [10,12]. The synthesis of AgNPs could be

* **Corresponding author: Muslikhin Hidayat,** Chemical Engineering Department, Gadjah Mada University, Jl. Grafika No. 2, Yogyakarta, 55281, Indonesia, e-mail: mhidayat@ugm.ac.id
Tintin Mutiara: Chemical Engineering Department, Gadjah Mada University, Jl. Grafika No. 2, Yogyakarta, 55281, Indonesia; Chemical Engineering Department, Universitas Islam Indonesia, Jl. Kaliurang km. 14.5, Yogyakarta, 55584, Indonesia
Hary Sulistyo, Moh. Fahrurrozi: Chemical Engineering Department, Gadjah Mada University, Jl. Grafika No. 2, Yogyakarta, 55281, Indonesia

done with the help of microorganisms [5,8] and plant extracts [9–11,13,14]. The microorganisms and plant extracts play a role of reducing and capping agent in forming of AgNPs [11,13,15]. The advantages of this method are that they are simple, environmentally friendly, inexpensive, and the application of non-toxic reactants [13] compared to the conventional processes. On the other hand, AgNPs' usage is limited by their stability depending on the surface charge of the suspending media and its rapid oxidation [16]. As a result, AgNPs have been integrated into composites to improve their stability and overcome rapid oxidation [17].

Recent studies proved that AgNPs could be impregnated into BC matrix via *in-situ* [18,19] or *ex-situ* synthesis [20,21]. In general, reductant chemicals are needed to reduce Ag^+ from bulk solution into Ag^0 of AgNPs and cap them in cellulose matrix for better stability, for example, adding sodium borohydride ($NaBH_4$) [8,15,22,23], triethanolamine (TEA) [24], and urea [25] to produce cellulose-AgNPs composites. To avoid the utilization of chemicals that may be hazardous to the environment, Han et al. [25] explained that cellulose was capable of reducing Ag^+ to Ag^0 at room temperature in strong alkali conditions. Also, the existence of alkali residue promotes the generation of Ag_2O, which was a deposit in the cellulose matrix and gave another easier reaction route to form AgNPs. Besides, the abundant hydroxyl group of BC itself was sufficient to supply the energy required for metal reduction [15].

BC has vast potential in many sectors because of its superior characteristics. However, the applications of BC on a large scale are constrained by its relatively low productivity and high cost of culture medium. The focus of this present study was to synthesize BC in a relatively low-cost medium and utilize it for the embedding and dispersion of AgNPs. *Acetobacter xylinum* strain grown in a simple coconut water medium was sterilized beforehand and used as a template for reducing and capping AgNPs. This method was simple, low cost, and used reduced chemicals, which has not been investigated. The most notable benefit of this study was providing sustainable nanoparticles composite biomaterials to meet the need for environmentally friendly products and utilize cheap and native resources. The resulting AgNPs templated BC products were characterized by Fourier transform infra-red (FTIR) to confirm the functional groups that play a role in forming and binding AgNPs in the BC matrix, X-ray diffraction (XRD), scanning electron microscope (SEM), and energy dispersive X-ray (EDX) to confirm the presence of AgNPs in BC matrix. The thermal stability of AgNPs templated BC was also assessed by thermogravimetric analysis (TGA). The antibacterial activities were measured by the inhibition zone of gram-positive bacteria (*S. aureus*) and gram-negative bacteria (*E. coli*).

2 Materials and methods

2.1 Materials

Silver nitrate ($AgNO_3$), sodium hydroxide (NaOH), and acetic acid glacial (CH_3COOH) were analytical grades and purchased from Merck, Germany. The coconut water was supplied by the local market in Yogyakarta, Indonesia. The white sugarcane crystals were purchased from PT. Sweet Indo Lampung, Indonesia, and $(NH_4)_2SO_4$ were purchased from PT. Petrokimia Gresik, Indonesia.

2.2 Preparation and purification of BC

BC from coconut water, commonly known as *nata de coco*, was produced by boiling 1 L of coconut water, 10 g sugarcane, and 5 g $(NH_4)_2SO_4$. Acetic acid was added dropwise to adjust the pH of the solution to 5.0. After the coconut water medium cooled down, about 10 mL of *Acetobacter xylinum* solution starter was added, then the solution was left for fermentation at room temperature for 4 days. BC produced was harvested and rinsed with running water until the pH of the rinsing water became neutral. BC was then put in boiling water for 5 min to kill the remaining bacteria. The resulting BC sheet with a thickness of 4 mm, as seen in Figure 1, was immersed in distilled water and stored at 4°C until subsequent use.

2.3 Impregnation of Ag into BC matrix

The BC sheet obtained initially was treated by soaking in various concentrations of $AgNO_3$ solution (2, 5, 10, and 15 mM) with constant mixing for 1 h, then leaving it to rest for a night to make sure the Ag^+ ions fully adsorb into the BC matrix. BC sheet treated with $AgNO_3$ was then rinsed with distilled water for 5 min to eliminate the excess $AgNO_3$ solution, followed by reduction process by immersing in 0.01 N NaOH solution for 10 min. Browny BC sheet indicated the formation of AgNPs in the BC matrix [8,23,25]. AgNPs templated BC was then dried in Memmert oven at 60°C until dry sheet was obtained (±2 h).

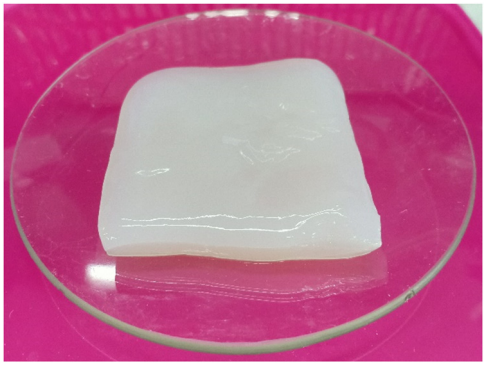

Figure 1: Bacterial cellulose *nata de coco* fermented for 4 days.

The composite sheet of AgNPs templated BC was denoted as AgNP2@BC, AgNP5@BC, AgNP10@BC, and AgNP15@BC according to the concentration of $AgNO_3$ used for the treatment at the initial stage.

2.4 Characterization of AgNPs templated BC

FTIR data were collected using the Nicolet Avatar 360 IR instrument, measured at a wavelength of 4,000–500 cm^{-1}. XRD pattern of pristine BC and AgNP@BC was identified using the Bruker D2 Phaser X-ray Diffraction instrument with a value of 2θ from 10° to 80°. The crystallinity index (CI) was measured as:

$$\mathrm{CI} = \frac{(I_{002} - I_{\mathrm{am}})}{I_{002}} \times 100\% \quad (1)$$

where I_{002} is the maximum intensity, and I_{am} is the intensity of the amorphous region [26]. Surface morphology and elemental composition of AgNPs templated BC were seen using SEM-EDX Phenom Desktop ProXL. The presence of AgNPs in the BC matrix was measured by TGA Linseis PT1000 with an analytical temperature from 0°C to 600°C, heating rate value of 10°C·min^{-1}, and nitrogen gas flow rate of 50 mL·min^{-1} to avoid degradation of the sample by thermal oxidation.

2.5 Assay of antibacterial activity

The potential antibacterial activity of AgNP@BC was measured by gram-positive bacteria (*S. aureus*) and gram-negative bacteria (*E. coli*). For this investigation, bacteria were grown in agar nutrients placed in a 10 cm diameter Petri dish. First, a nutrient agar medium was prepared with a concentration of 20 g·L^{-1}. Agar medium was sterilized at 121°C for 15 min. After the agar medium was cooled at 40°C, bacteria were inoculated up to 10^7. Agar medium was then stirred until homogeneous, poured into a Petri dish (±20 mL), and left until hardened. A small piece of AgNPs templated BC was placed on the surface of the agar medium. This Petri dish was cooled at 4–10°C for 1 h and then incubated at 37°C for 24 h (or until the inhibition zone was clearly visible). The formation of the inhibition zone was then measured for each sample.

3 Results and discussion

3.1 Impregnation of Ag into BC matrix

BC is produced from the fermentation process of sugars, especially fructose and glucose, by exopolysaccharide-producing bacteria [27]. Coconut water was selected as the primary ingredient in the fermentation media in this study because it contains nutrients and minerals that *Acetobacter xylinum* needs for metabolism [28]. During fermentation, *Acetobacter xylinum* converts sucrose into glucose and fructose with the help of the sucrase enzyme and produces a white sheet of cellulose due to metabolism activities. The thickness of the resulting BC membrane increased with the increase in the fermentation time [29]. After 4 days of fermentation, a milky white BC sheet with a thickness of 4 mm was formed, as shown in Figure 1.

Wet BC sheets were immersed in distilled water at 4°C for several days to obtain a consistent grey or brown color when impregnated in $AgNO_3$ solution. This step was done to ensure that the BC pores were completely filled with water so that when the BC sheet was immersed in $AgNO_3$ solution, it was expected that Ag particles would be easier to fill in the BC matrix. The immersion of the BC sheet in the $AgNO_3$ solution was carried out for a day to ensure that Ag ions were completely adsorbed in the BC matrix. Abundant hydroxyl groups in BC can reduce Ag ions and provide anchoring sites for Ag^+ [5]. After the immersion step, the BC sheet looks slightly blackish, as seen in Figure 2a. The following process was immersion in 0.01N NaOH solution to facilitate strong alkaline conditions, so the BC could reduce Ag^+ to Ag^0 and simultaneously produce AgNPs, which is capped in the BC matrix [25]. After immersion in NaOH solution, the BC sheet turned brownish in color (Figure 2b), indicating the formation of AgNPs [8,23,25].

The formation of AgNPs can be explained as an interaction with the hydroxyl groups of cellulose. The diffusion of hydrated silver ions $(Ag(H_2O)_2)^+$ to the BC matrix

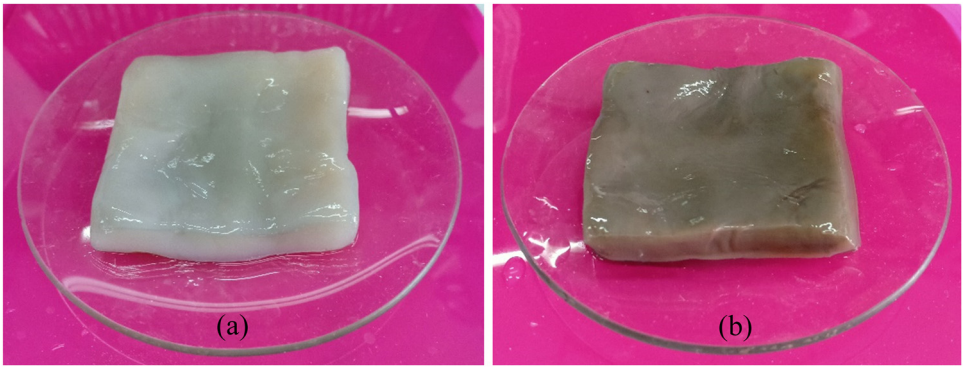

Figure 2: Bacterial cellulose *nata de coco*: (a) immersed in $AgNO_3$ solution and (b) reduced by NaOH solution.

leads to coordination with the hydroxyl groups of cellulose [24]. This can be indicated by FTIR spectra. Once the AgNPs are made, the BC matrix forms a thin layer or film that acts as a capping agent, stabilizer, and agglomeration preventer [30]. In the end, AgNPstemplated BC with a small and tight size distribution was obtained. The final step was to dry the sheet in an oven at 60°C to obtain a dry sheet.

3.2 FTIR analysis

FTIR analysis was carried out to ascertain the spectrum shift indicating the functional groups that play a role in forming and binding AgNPs in the BC matrix structure. FTIR spectra of pristine BC and AgNPs templated BC is presented in Figure 3.

FTIR spectra of both the pristine BC and AgNP@BC in Figure 3 showed the typical spectrum of cellulose. The spectrum detected around 3,400–3,600 cm^{-1} in both the graphs indicated an abundance of OH group, which may play a significant role in reducing Ag^+ from $AgNO_3$ to Ag^0 of AgNPs and stabilizing AgNPs in the BC matrix by acting as a capping agent [23,30,31], and also hydroxyl groups have been shown to have the ability to coordinate with metal ions. As a result of reducing Ag^+ ions in the BC matrix, AgNP@BC FTIR spectra exhibited spectrum shift from 2,792 to 2,804 cm^{-1} corresponding to the shift of carbonyl group of aldehyde group. Additionally, a spectrum appeared at 1,714 cm^{-1} assigned to C═O of the carbonyl group. These significant spectrum changes in the FTIR spectrum reflected the considerable factors in the synthesis of metal nanoparticles: the oxidation of hydroxyl and aldehyde groups to form carbonyl groups [30,31]. Previously published studies also stated that the band appearing in the range of 1,700–1,600 cm^{-1} indicated the formation of AgNPs capped in biostructure [11,32,33].

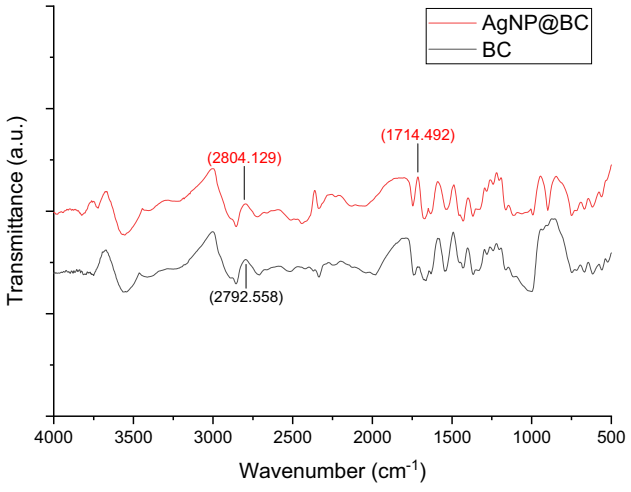

Figure 3: FTIR spectra of pristine BC and sample AgNP10@BC.

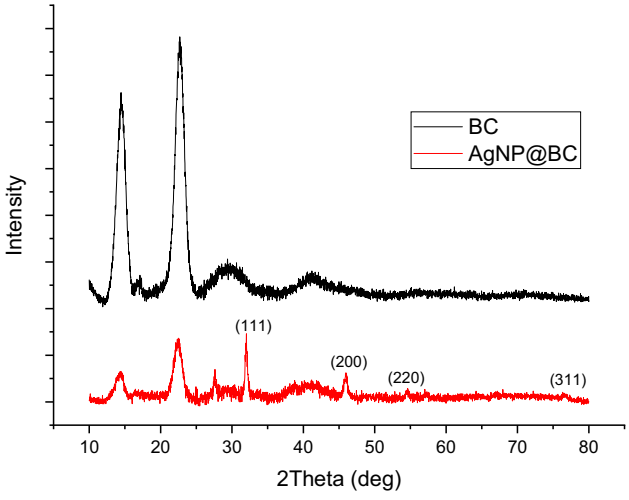

Figure 4: XRD graph of pristine BC and AgNP10@BC.

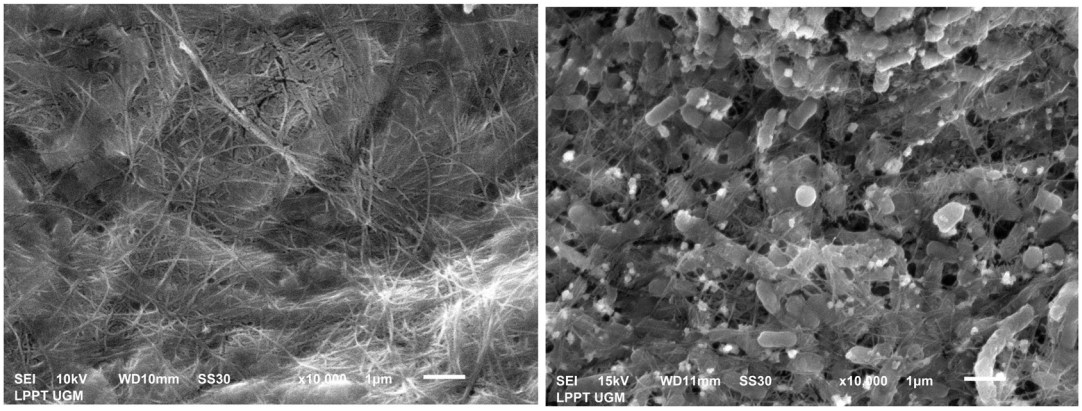

(a) (b)

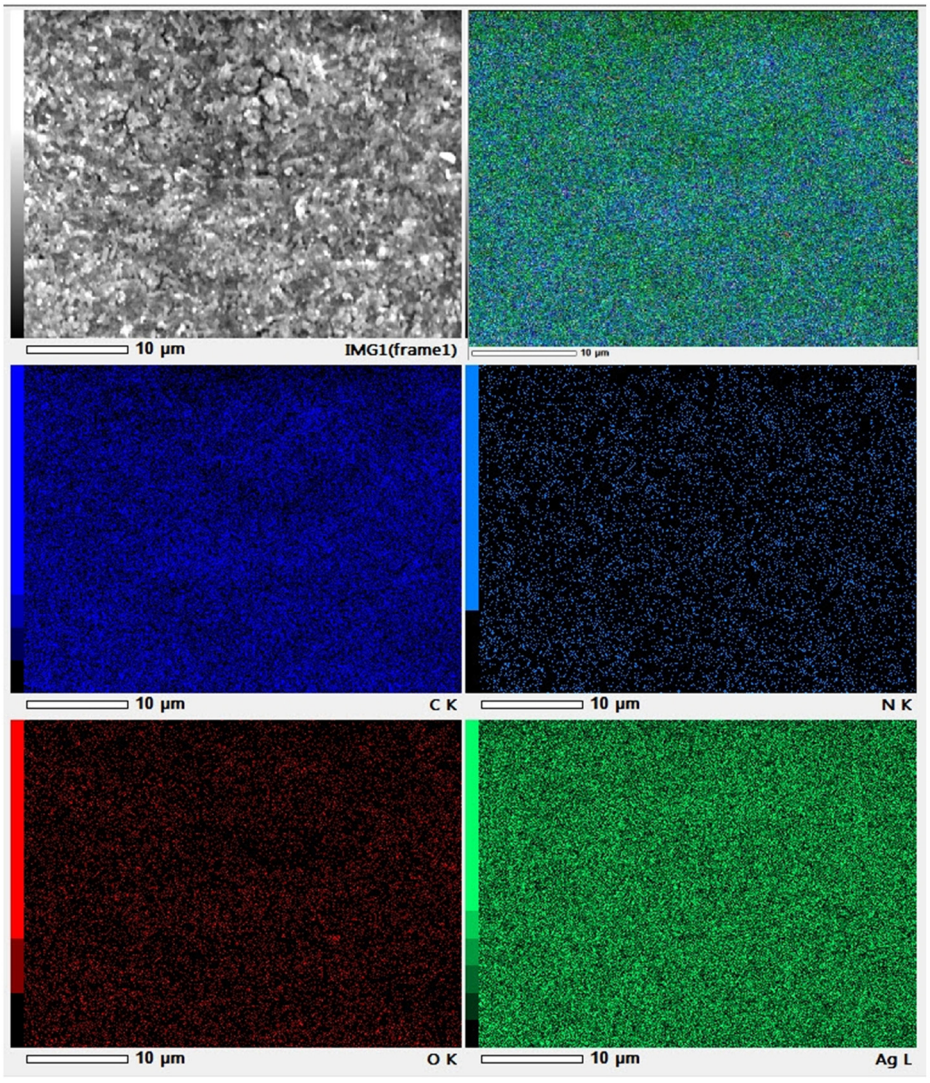

(c)

Figure 5: SEM image of: (a) pristine BC, (b) AgNP15@BC, and (c) its elemental mapping.

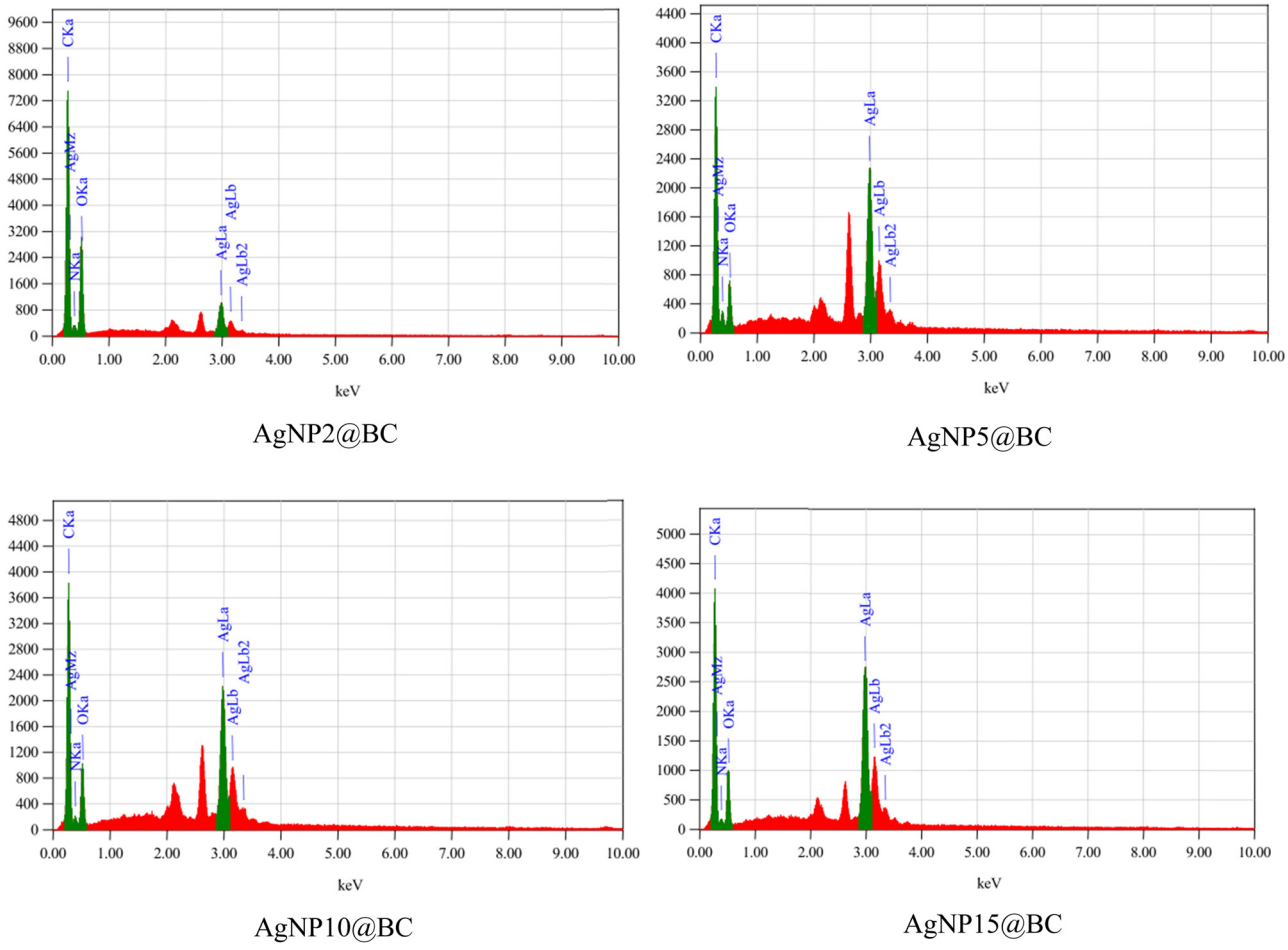

Figure 6: EDX quantitative analysis of AgNPs templated BC.

Table 1: Elements detected in AgNPs templated BC samples by EDX analysis

Sample	Element (%)			
	Ag	C	O	N
AgNP2@BC	8.13	37.55	33.48	20.83
AgNP5@BC	31.36	28.09	17.39	23.16
AgNP10@BC	28.74	30.47	22.42	18.37
AgNP15@BC	33.21	29.15	20.78	16.86

3.3 X-ray diffraction

XRD analysis indicates the crystal structure, crystallinity index, and silver content of the BC matrix. Diffraction was measured at 2θ value from 10° to 80°. Diffraction peaks of pristine BC and AgNPs templated BC are shown in Figure 4.

Those diffraction peaks showed the pattern of typical cellulose I. Diffraction of BC showed prominent peaks

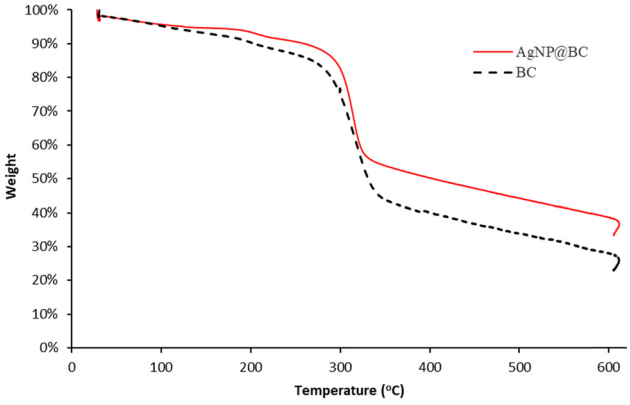

Figure 7: Thermal stability of pristine BC and AgNP10@BC by TGA analysis.

at 2θ = 14.46° which correspond to triclinic structure (Iα) = 110 and monoclinic structure (Iβ) = 100, 17.11° which correspond to Iα = 010 and Iβ = 110, and 22.69° which correspond to Iα = 110 and Iβ = 200 [34,35]. The

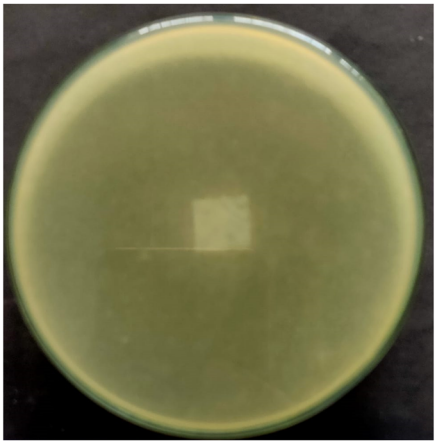

(a)

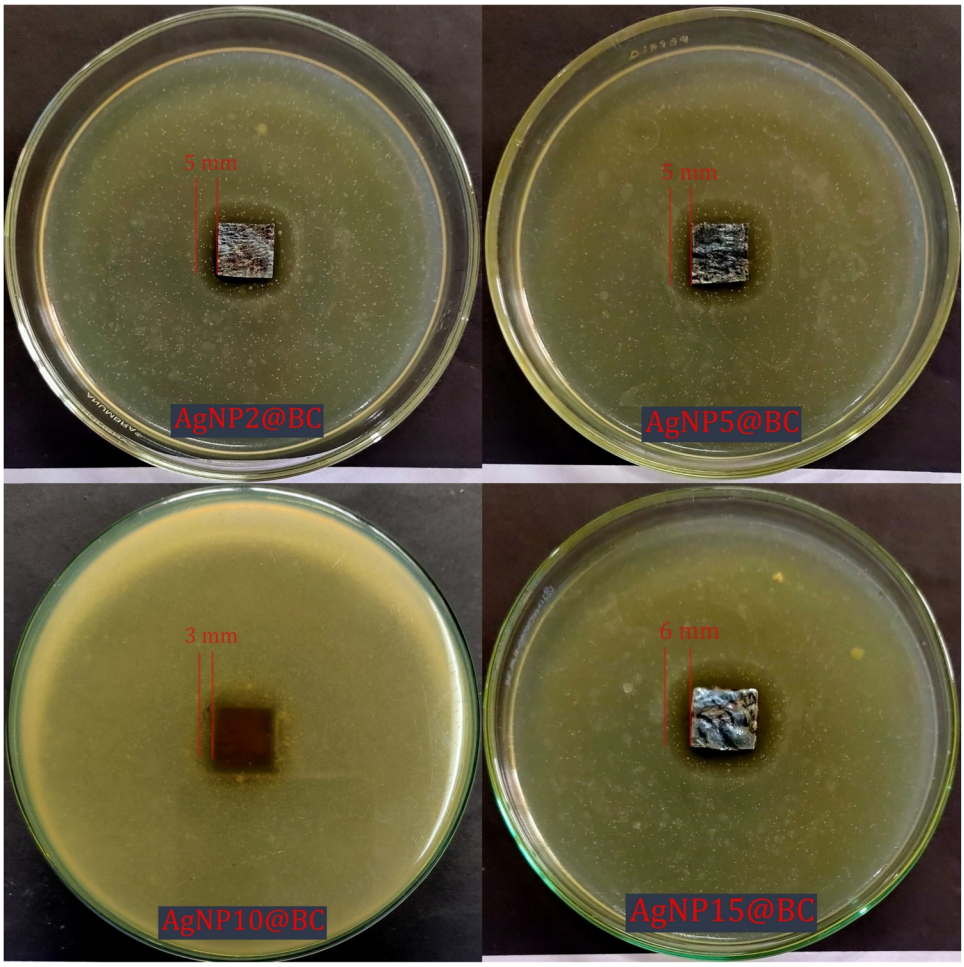

(b)

Figure 8: Antibacterial activity against *S. aureus* of: (a) pristine BC and (b) AgNPs templated BC.

diffraction peaks of AgNP@BC at 32.04°, 45.9°, 54.4°, and 78.36° corresponded to the lattice plane values (111), (200), (220), and (311) of a face centered cubic (FCC) metallic silver crystal fitted with a JCPDS card of Ag (No. 4-783) [10,11,36], demonstrating the presence of AgNPs in the BC matrix. These samples' crystallinity index (CI) was 73.47% for pristine BC and 72.57% for AgNPs templated BC. These results were conformable with crystallinity index data for BC

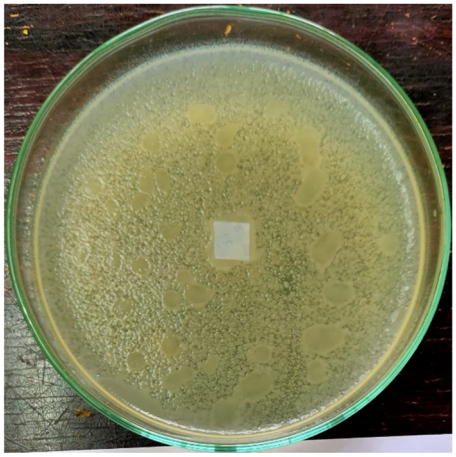

(a)

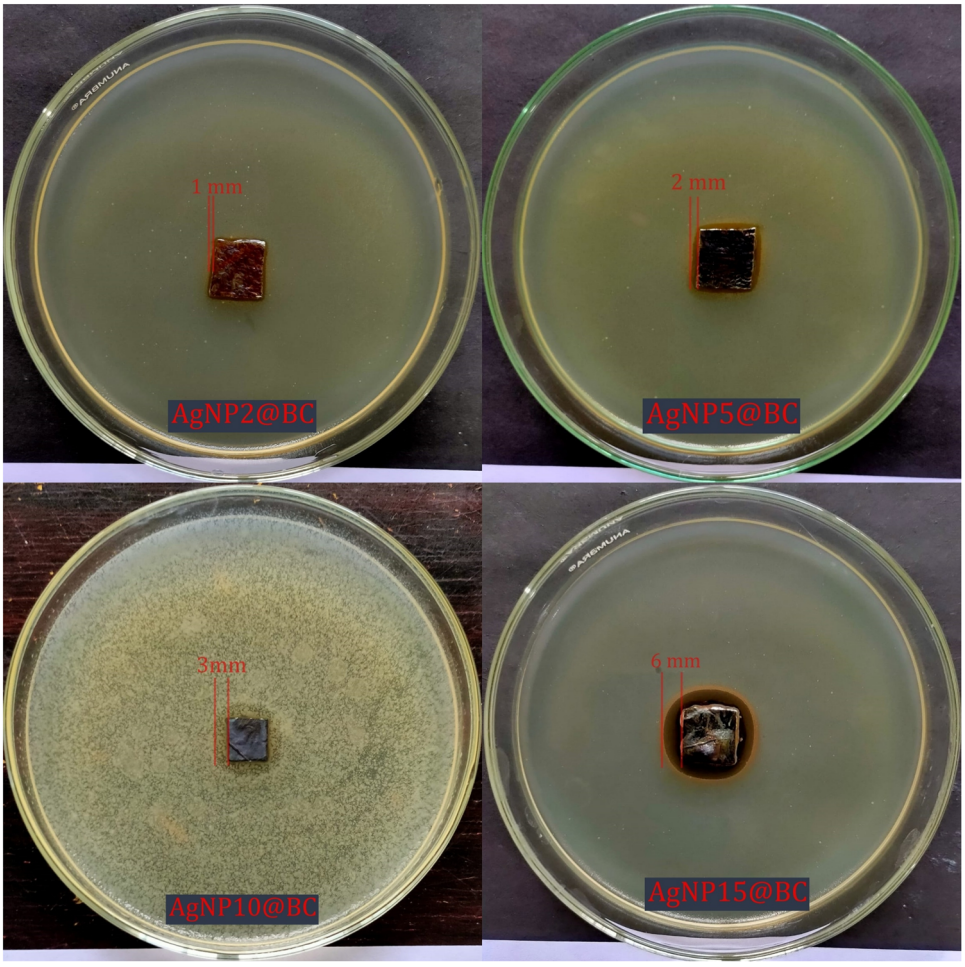

(b)

Figure 9: Antibacterial activity against *E. coli* of: (a) pristine BC and (b) AgNPs templated BC.

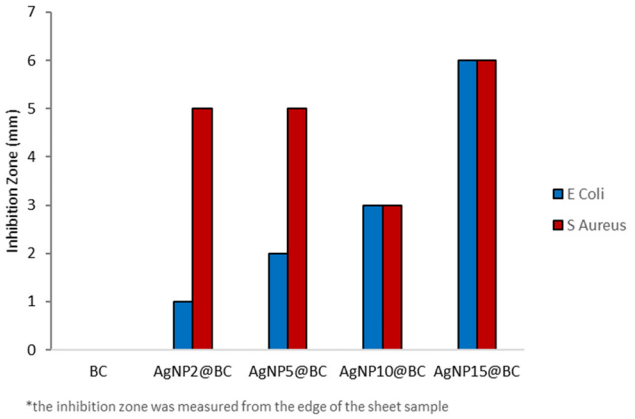

Figure 10: Inhibition zone of BC and AgNPs templated BC against *S. aureus* and *E. coli*.

products from previously published articles [3,35,37] and indicated that deposition of AgNPs did not affect the crystal structure of BC.

3.4 Morphology of AgNP templated BC

SEM analysis was performed to obtain the morphological surface information. As seen in Figure 5, it was shown that pristine BC was composed of nanofiber networks that form evenly distributed micro spaces. The typical network structure of BC is all dependent on porosity, compaction, and water tightness [3]. All studies reveal that the morphology BC was composed of a homogeneous network of cellulose microfibrils as presented in Figure 5a, similar to those reported in previous studies [37,38]. Meanwhile, the AgNPs templated BC sample showed spherical (white dot) AgNPs embedded between the nanofiber networks of BC as presented in Figure 5b. The spherical AgNPs formed in the BC matrix depend on the porosity and surface crystallography [8,9,15,24].

EDX scanning can be used to determine the elements and chemical composition of a material. The presence of AgNPs embedded in the BC matrix was clearly visualized in EDX mapping, as presented in Figure 5c. Additionally, EDX quantitative analysis was done to determine the concentration of AgNPs in the BC matrix. As illustrated in Figure 6, a strong peak at 3 keV of EDX quantitative analysis confirmed the presence of AgNPs. Table 1 summarizes the elements found in AgNPs templated BC based on the EDX analysis. The maximum Ag content was possessed by the AgNP15@BC sample with 33.21% mass, the remaining components, including C, O, and N, were derived from the BC sheet. This result is in accordance with the thermal stability data, which confirmed that there was 33% mass residue of AgNPs templated BC sample after heating up to 600°C indicating the presence of AgNPs.

3.5 Thermal stability

TGA was performed to investigate the thermal stability of BC and AgNPs templated BC sheets. The results are displayed in Figure 7.

The first significant weight loss occurred when heated up to 100°C. The remaining weight of both the BC and

Table 2: Comparison of antibacterial activity of several AgNP/BC composite materials

BC	Synthesis method	Antibacterial activity	References
Gluconacetobacter xylinus grown in medium containing mannitol, tryptone, and yeast extract	UV irradiation	Inhibition zone of 6.5 mm against *S. aureus*	[19]
Acetobacter xylinum grown in medium containing D-glucose anhydrous, yeast extract powder, and distilled water	$NaBH_4$ reduction	Inhibition zone of 2 mm against *E. coli* and 3.5 mm against *S. aureus*	[22]
Gluconacetobacter intermedius grown in HS medium	TEMPO oxidation, followed by sodium citrate reduction	Inhibition zone of 3.7 mm against *E. coli* and 3.2 mm against *S. aureus*	[40]
Gluconacetobacter xylinum grown in HS medium	TEMPO oxidation	Diameter of inhibition area was 19 mm in *V. harveyi* and 21 mm in *V. parahaemolyticus*	[18]
Komagataeibacter xylinus grown in medium containing glucose, yeast extract, KH_2PO_4, $MgSO_4{\cdot}7H_2O$, and ethanol	Montmorillonite incorporation	Inhibition zone of 2.0 mm for *S. aureus* and 2.5 mm for *P. aeruginosa*	[21]
Acetobacter xylinum grown in coconut water medium	Alkali reduction	Inhibition zone of 6 mm against both *E. coli* and *S. aureus*	This study

AgNPs templated BC sheets was 95%. This weight loss happened due to the evaporation of the remaining water in the BC matrix. The subsequent significant weight loss occurred at 270°C, which may be associated with the degradation of cellulose, including depolymerization, dehydration, and decomposition of glucose units [3]. When heated over 600°C, around 20% of the remaining weight of the BC sample corresponded to burnt ashes, similar to the other reported studies [3,34,38]. Based on the TGA curve in Figure 7, AgNPs' presence can be detected as the residue around 33% on heating above 600°C. The residue may be attributed to the remaining ashes from combustion and silver particles which do not degrade due to heating. Based on this investigation, both the pristine BC and AgNPstemplated BC were relatively stable at thermal heating up to 250°C. Considering the requirement for industrial application materials that remain intact at high temperatures of 250°C [3], this BC exhibits good thermal stability. Thermal degradation is one of the critical criteria of BC as a biopolymer for industrial material. Characteristic of the BC such as crystallinity, molecular weight, hydrophilicity, and functionalized with an inorganic nanoparticle are primary factors that could affect the thermal degradation of BC [39].

3.6 Antibacterial activities

Recently, AgNPs have been applied as antibacterial agents for several commercial products such as food storage, body care, pharmaceuticals, water treatment, and paint [10]. The antibacterial activity of pristine BC and AgNPs templated BC was measured by the inhibition zone of gram-positive bacteria (*S. aureus*) and gram-negative bacteria (*E. coli*), presented in Figures 8 and 9.

The visual difference of agar media for each sample was caused only by incubation and observation time. The incubation time does not directly affect the inhibition zone, so this visual difference could be neglected. During this incubating time, bacteria grew normally in the area around the pristine BC. On the other hand, the inhibition zone was clearly formed around AgNPs templated BC. The antibacterial strength of AgNPs templated BC against *S. aureus* (Figure 8b) and *E. coli* (Figure 9b) were tested with different concentrations of $AgNO_3$ solution, which were used in the initial treatment of synthesis of AgNPs templated BC. The concentration of $AgNO_3$ solution affects the antibacterial strength of the sheet. It was observed that AgNP15@BC has the maximum antibacterial activity against both *S. aureus* and *E. coli*. Figure 10 exhibited a bar diagram of the inhibition zone formed by each sample, which proved that AgNPs templated BC generated a larger inhibition zone against gram-positive bacteria compared to gram-negative bacteria.

Previous studies demonstrated that AgNP/BC composites were effective in controlling pathogenic bacteria such as *E. coli* [22,40], *S. aureus* [19,21,22,40], *P. aeruginosa* [21], *V. harveyi*, and *V. parahaemolyticus* [18]. A similar result was obtained in this study where the AgNPs templated BC showed a good antibacterial activity compared to previously published studies, as shown in Table 2. It was noticeable that AgNPs templated BC is a potential material for the antibacterial application and could be effectively utilized in pharmaceutical, biotechnological, and biomedical applications.

4 Conclusion

Investigation of synthesis of AgNPs templated BC sheet as a potential material for the antibacterial and industrial application has been done. The AgNPs templated BC was prepared via a simple and greener route. This work demonstrates that Ag ions in 2–15 mM $AgNO_3$ solution can successfully be incorporated into BC matrix as AgNPs with the help of reducing in 0.01N NaOH solution. The presence of AgNPs in the BC matrix was verified by FTIR, XRD, SEM, EDX, and TGA analyses. In addition, the presence of AgNPs in the BC matrix showed the antibacterial activity on both *S. aureus* and *E. coli*, which is relevant for controlling pathogenic bacteria related to several human diseases. Finally, synthesis of BC from *Acetobacter xylinum* grown in coconut water medium and utilized as a template for the formation of AgNPs provides a low-cost and straightforward method for developing biomaterial for antibacterial and industrial applications.

Acknowledgment: All authors gratefully acknowledge the Directorate of Research and Community Service, Gadjah Mada University, for funding this research project.

Funding information: This work was funded by the Directorate of Research and Community Service, Gadjah Mada University, under contract number 3143/UN1.P.III/DIT-LIT/PT/2021 (final assignment recognition 2021).

Author contributions: Tintin Mutiara: writing – original draft, conceptualization, methodology, investigation, and visualization; Hary Sulistyo: writing – review, investigation, and supervision; Moh. Fahrurrozi: writing – review, investigation, and supervision; Muslikhin Hidayat:

writing – review, conceptualization, investigation, supervision, project administration, and funding acquisition.

Conflict of interest: Authors state no conflict of interest.

References

[1] Sai H, Jin Z, Wang Y, Fu R, Wang Y, Ma L. Facile and green route to fabricate bacterial cellulose membrane with superwettability for oil–water separation. Adv Sustain Syst. 2020;4(7):1–9.

[2] Wang J, Tavakoli J, Tang Y. Bacterial cellulose production, properties and applications with different culture methods – A review. Carbohydr Polym. 2019;219:63–76.

[3] Galdino CJS, Maia AD, Meira HM, Souza TC, Amorim JDP, Almeida FCG, et al. Use of a bacterial cellulose filter for the removal of oil from wastewater. Process Biochem. 2019;1:288–96.

[4] Lehtonen J, Chen X, Beaumont M, Hassinen J, Orelma H, Dumée LF, et al. Impact of incubation conditions and post-treatment on the properties of bacterial cellulose membranes for pressure-driven filtration. Carbohydr Polym. 2020;251:51.

[5] Yang Y, Chen Z, Wu X, Zhang X, Yuan G. Nanoporous cellulose membrane doped with silver for continuous catalytic decolorization of organic dyes. Cellulose. 2018;25(4):2547–58.

[6] Romling U, Galperin MY. Bacterial cellulose biosynthesis: diversity of operons, subunits, products and functions. Trends Microbiol. 2015;23(9):545–57.

[7] Tian D, Guo Y, Huang M, Zhao L, Deng S, Deng O, et al. Bacterial cellulose/lignin nanoparticles composite films with retarded biodegradability. Carbohydr Polym. 2021;274:118656.

[8] Yang G, Xie J, Hong F, Cao Z, Yang X. Antimicrobial activity of silver nanoparticle impregnated bacterial cellulose membrane: Effect of fermentation carbon sources of bacterial cellulose. Carbohydr Polym. 2021;87(1):839–45.

[9] Hamedi S, Shojaosadati AS, Mohammad A. Evaluation of the catalytic, antibacterial and anti-biofilm activities of the Convolvulus arvensis extract functionalized silver nanoparticles. J Photochem Photobiol B Biol. 2017;167:36–44.

[10] Renuka R, Devi KR, Sivakami M, Thilagavathi T, Uthrakumar R, Kaviyarasu K. Biosynthesis of silver nanoparticles using Phyllanthus emblica fruit extract for antimicrobial application. Biocatal Agric Biotechnol. 2020;24:101567.

[11] Chand K, Cao D, Eldin Fouad D, Hussain Shah A, Qadeer Dayo A, Zhu K, et al. Green synthesis, characterization and photocatalytic application of silver nanoparticles synthesized by various plant extracts. Arab J Chem. 2020;13(11):8248–61.

[12] Marimuthu S, Antonisamy AJ, Malayandi S, Rajendran K, Tsai PC, Pugazhendhi A, et al. Silver nanoparticles in dye effluent treatment: A review on synthesis, treatment methods, mechanisms, photocatalytic degradation, toxic effects and mitigation of toxicity. J Photochem Photobiol B Biol. 2020;205:111823.

[13] Khodadadi B, Bordbar M, Yeganeh-Faal A, Nasrollahzadeh M. Green synthesis of Ag nanoparticles/clinoptilolite using Vaccinium macrocarpon fruit extract and its excellent catalytic activity for reduction of organic dyes. J Alloy Compd. 2017;719:82–8.

[14] Ravichandran V, Vasanthi S, Shalini S, Shah SAA, Tripathy M, Paliwal N. Green synthesis, characterization, antibacterial, antioxidant and photocatalytic activity of Parkia speciosa leaves extract mediated silver nanoparticles. Results Phys. 2019;15:102565.

[15] Yang G, Xie J, Deng Y, Bian Y, Hong F. Hydrothermal synthesis of bacterial cellulose/AgNPs composite: A 'green' route for antibacterial application. Carbohydr Polym. 2012;87(4):2482–7.

[16] Hillenkamp M, Domenicantonio GD, Eugster O, Félix C. Instability of Ag nanoparticles in SiO_2 at ambient conditions. Nanotechnology. 2006;18:015702.

[17] Jeevanandam J, Krishnan S, Hii YS, Pan S, Chan YS, Acquah C. Synthesis approach-dependent antiviral properties of silver nanoparticles and nanocomposites. J Nanostruc Chem. 2022;1–23.

[18] Elayaraja S, Zagorsek K, Li F, Xiang J. *In situ* synthesis of silver nanoparticles into TEMPO-mediated oxidized bacterial cellulose and their antivibriocidal activity against shrimp pathogens. Carbohydr Polym. 2017;166:329–37.

[19] Yang G, Wang C, Hong F, Yang X, Cao Z. Preparation and characterization of BC/PAM-AgNPs nanocomposites for antibacterial applications. Carbohydr Polym. 2015;115:636–42.

[20] Nicoara AI, Stoica AE, Ene DE, Vasile BS, Holban AM, Neacsu I I*n situ* and *ex situ* designed hydroxyapatite: bacterial cellulose materials with biomedical applications. Mater (Basel). 2020;13(21):4793.

[21] Horue M, Cacicedo ML, Fernandez MA, Rodenak-Kladniew B, Torres Sánchez RM, Castro GR. Antimicrobial activities of bacterial cellulose – Silver montmorillonite nanocomposites for wound healing. Mater Sci Eng C. 2020;116:111152.

[22] Maneerung T, Tokura S, Rujiravanit R. Impregnation of silver nanoparticles into bacterial cellulose for antimicrobial wound dressing. Carbohydr Polym. 2008;72(1):43–51.

[23] Isik Z, Unyayar A, Dizge N. Filtration and antibacterial properties of bacterial cellulose membranes for textile wastewater treatment. Avicenna J Env Heal Eng. 2018;5(2):106–14.

[24] Barud HS, Barrios C, Regiani T, Marques RFC, Verelst M, Dexpert-Ghys J, et al. Self-supported silver nanoparticles containing bacterial cellulose membranes. Mater Sci Eng C. 2008;28(4):515–8.

[25] Han Y, Wu X, Zhang X, Zhou Z, Lu C. Reductant-Free Synthesis of Silver Nanoparticles-Doped Cellulose Microgels for Catalyzing and Product Separation. ACS Sustain Chem Eng. 2016;4(12):6322–31.

[26] Segal L, Creely JJ, Martin AE, Conrad CM. An empirical method for estimating the degree of crystallinity of native cellulose using the X-Ray diffractometer. Text Res J. 1959;29(10):786–94.

[27] Thakur K, Kumar V, Kumar V, Kumar S. Genomic characterization provides genetic evidence for bacterial cellulose synthesis by Acetobacter pasteurianus RSV-4 strain. Int J Biol Macromol. 2020;156:598–607.

[28] Barlina R, Palma B. Bioselulosa Dari Nata De Coco Sebagai Bahan Baku Edible Film. Kementrian Pertanian, Badan Litbang Pertanian. 2011 [cited 2021 April 23]. https://www.litbang.pertanian.go.id/info-teknologi/1915/file/Bioselulosa-dari-Nata-De-C.pdf.

[29] Luo H, Zhang J, Xiong G, Wan Y. Evolution of morphology of bacterial cellulose scaffolds during early culture. Carbohydr Polym. 2014;111:722–8.
[30] Escárcega-González CE, Garza-Cervantes JA, Vázquez-Rodríguez A, Morones-Ramírez JR. Bacterial exopolysaccharides as reducing and/or stabilizing agents during synthesis of metal nanoparticles with biomedical applications. Int J Polym Sci. 2018;2018:1–15.
[31] Dong H, Snyder JF, Tran D, Leadore J. Hydrogel, aerogel and film of cellulose nanofibrils functionalized with silver nanoparticles. Carbohydr Polym. 2013;95:760–7.
[32] Sharma P, Pant S, Rai S, Yadav RB, Dave V. Green synthesis of silver nanoparticle capped with allium cepa and their catalytic reduction of textile dyes: an ecofriendly approach. J Polym Env. 2017;26:1795–803.
[33] Sathishkumar P, Preethi J, Vijayan R, Yusoff ARM, Ameen F, Suresh S, et al. Anti-acne, anti-dandruff and anti-breast cancer efficacy of green synthesized silver nanoparticles using Coriandrum sativum leaf extract. J Photochem Photobiol. 2016;B163:69–76.
[34] Leonarski E, Cesca K, Zanella E, Stambuk BU, de Oliveira D, Poletto P. Production of kombucha-like beverage and bacterial cellulose by acerola byproduct as raw material. Lwt. 2020;135:1–8.
[35] He F, Yang H, Zeng L, Hu H, Hu C. Production and characterization of bacterial cellulose obtained by Gluconacetobacter xylinus utilizing the by-products from Baijiu production. Bioprocess Biosyst Eng. 2020;43:0123456789-936.
[36] Jiang X, Xie Y, Lu J, Zhu L, He W, Qian Y. Preparation, characterization, and catalytic effect of CS2-stabilized silver nanoparticles in aqueous solution. Science. 2001;D21:3795–9.
[37] Gomes FP, Silva NH, Trovatti E, Serafim LS, Duarte MF, Silvestre AJ, et al. Production of bacterial cellulose by Gluconacetobacter sacchari using dry olive mill residue. Biomass Bioenergy. 2013;55:205–11.
[38] Corzo Salinas DR, Sordelli A, Martínez LA, Villoldo G, Bernal C, Pérez MS, et al. Production of bacterial cellulose tubes for biomedical applications: Analysis of the effect of fermentation time on selected properties. Int J Biol Macromol. 2021;189:1–10.
[39] Torgbo S, Sukyai P. Biodegradation and thermal stability of bacterial cellulose as biomaterial: The relevance in biomedical applications. Polym Degrad Stab. 2020;179:109232.
[40] Feng J, Shi Q, Li W, Shu X, Chen A, Xie X, et al. Antimicrobial activity of silver nanoparticles *in situ* growth on TEMPO-mediated oxidized bacterial cellulose. Cellulose. 2014;21:4557–67.